

DOrA: 3D Visual Grounding with Order-Aware Referring

Tung-Yu Wu¹, Sheng-Yu Huang¹, and Yu-Chiang Frank Wang^{1,2}

¹ National Taiwan University
 {b08901133, f08942095}@ntu.edu.tw
² NVIDIA
 frankwang@nvidia.com

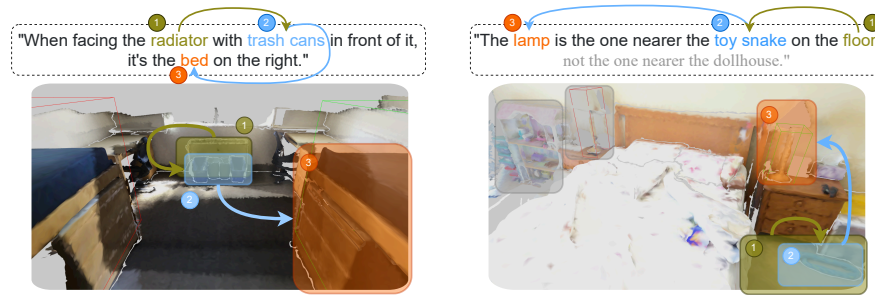


Fig. 1: Referential orders for 3D grounding. The order manifests an anchor-to-target referring process that helps identify the target object referred by the description.

Abstract. 3D visual grounding aims to identify the target object within a 3D point cloud scene referred to by a natural language description. While previous works attempt to exploit the verbo-visual relation with proposed cross-modal transformers, unstructured natural utterances and scattered objects might lead to undesirable performances. In this paper, we introduce DOrA, a novel 3D visual grounding framework with **Order-Aware** referring. DOrA is designed to leverage Large Language Models (LLMs) to parse language description, suggesting a referential order of anchor objects. Such ordered anchor objects allow DOrA to update visual features and locate the target object during the grounding process. Experimental results on the NR3D and ScanRefer datasets demonstrate our superiority in both low-resource and full-data scenarios. In particular, DOrA surpasses current state-of-the-art frameworks by 9.3% and 7.8% grounding accuracy under 1% data and 10% data settings, respectively.

Keywords: 3D Computer Vision · 3D Visual Grounding

1 Introduction

Visual grounding is an emerging task that aims to ground a target object in a given 2D/3D scene from a natural description, where the description contains information to identify the target object (e.g., color, shape, or relations to other anchor objects). This task is potentially related to industrial applications to

AR/VR and robotics [3,25,27]. Compared to object detection, the main challenge of visual grounding lies in the requirement to find *the only one* object described in the given natural description, while there might be multiple objects with the same class of the target object appearing in the scene. Therefore, the model is expected to identify the relations between all objects in the scene to find the ideal target object according to the given description. In recent years, significant progress has been made in image-based 2D visual grounding [23,29,38,45,51,54]. However, comparatively fewer efforts are directed towards addressing the more intricate challenge of 3D visual grounding, raised from joint consideration of the unstructuredness of natural language descriptions and scattered object arrangements in the 3D scene. The complications of the two modalities make it challenging to directly refer to the target object with plain cross-modal interaction between the features of the scene point cloud and the referring description, showing the need for additional research in the field of 3D visual grounding.

As pioneers of 3D visual grounding, Referit3D [2] and ScanRefer [8] are two benchmark datasets that build upon the point cloud scene provided by the ScanNet [12] dataset. The former presents a graph neural network (GNN) [36]-based framework to explicitly learn the object spatial relations as the baseline. The latter designs a verbo-visual cross-modal feature extraction and fusion pipeline as the baseline. Several subsequent methods are presented [4,11,15,19–21,31,40,46], which either augment the visual features [4,20,31,46], utilize specialized cross-modal feature alignment frameworks [21], or exploit spatial relations with designed frameworks/modules [11,15,17,19,40] are proposed to solve the 3D visual grounding problem. However, these approaches use a referring head to localize the target object directly. Without explicitly considering any additional information about the anchor objects mentioned in the description, models must implicitly discover the relation between the anchor objects and the target object. They may be misled by other similar objects presented, as pointed out in [5]. To overcome this issue, some approaches [1,42,49] propose to incorporate anchor objects during training by including their label annotations [5,18]. Nonetheless, human annotators are usually required to obtain this additional linguistic information [1,49], causing potential difficulty in scaling up to larger datasets for real-world applications.

To unload the need for human annotators, recent approaches [5,18] leverage large language models (LLMs) for automatic dissection of the descriptions and generation of prior linguistic knowledge. For example, NS3D [18] utilizes Codex [10] to parse descriptions into nested expressions and designs a neuro-symbolic framework to find the target object step-by-step. However, NS3D is restricted to fixed-template relations between objects (e.g., below/above, near/far, etc.) and cannot be easily extended to arbitrary natural descriptions. Inspired by the mechanism of human perception system [9,32], CoT3DRef [5] generates the referential order of a description that points from anchor objects to the final target object. For example, for a description “*Find the water bottle on the table nearest to the door.*”, the referential order is generated as { “*door*” (anchor), “*table*” (anchor), “*water bottle*” (target) }. A rule-based algorithm is presented

to establish matching between each class name in the referential order and a corresponding anchor/target object in the scene at once, with the matching results being used to guide a transformer-based module to predict the final target object. However, if the matching results calculated by the rule-based method are not accurate, the performance might be degraded.

In this paper, we propose a **3D Visual Grounding Framework with Order-Aware Referring (DOrA)**. By utilizing a Large Language Model (LLM) of GPT-3.5-Turbo [48], DOrA exploits the awareness of anchor objects with the associated referential order from the textual description, as depicted in Fig. 1. With this referential order of anchor objects as guidance, a series of Object Referring blocks is deployed in DOrA to process the extracted anchor/target objects, each performing feature enhancement to update the visual features of corresponding objects. Since only the ground-truth identity of the target object is available during training (no ground-truth referential order observed), we additionally introduce a pre-training strategy to augment *accurate* labels and referential orders for anchor/target objects. By conducting extensive experiments on real-world benchmark datasets, we show that our DOrA is comparable to current state-of-the-art 3D visual-grounding methods on the standard setting and further outperforms them significantly when training data is limited.

We now summarize our contribution as follows:

- We present a 3D Visual Grounding Framework with **Order-Aware Referring (DOrA)** for 3D visual grounding via natural descriptions.
- With a two-stage in-context learning technique on LLM, DOrA infers a series of anchor/target objects in a referential order to guide the grounding process.
- DOrA deploys a series of Object-Referring blocks that follows the referential order and progressively refines the features of anchor/target objects for improved groundings.
- A pre-training scheme is introduced for DOrA, which augments reliable labels and accurate referential orders of anchor/target objects as additional training examples, ensuring the awareness of the identities and referential orders of anchor objects.

2 Related Work

2.1 2D Visual Grounding

2D visual grounding aims to locate the target object in an image referred to by a natural language description, with various approaches being proposed in recent years [23, 28, 29, 38, 39, 45, 47, 51]. Among them, verbo-visual feature alignment frameworks [23, 28, 29, 51] have proven themselves to be an effective way to equip models with abilities of tackling description contexts and image semantics simultaneously. Particularly, as one of the pioneers, MDETR [23] extends DETR [7], an end-to-end object detection framework, to incorporate text modalities with the proposed text-image alignment contrastive losses. GLIP [51] takes a step forward to improve the performance of visual grounding by proposing

unified multi-task learning that includes object localization and scene understanding tasks, showing that these tasks could gain mutual benefits from each other. Grounding DINO [29] further designs the large-scale grounding pretraining for DINO [16], reaching the capability of open-set grounding. Although great progress is achieved, extending these 2D visual grounding methods to 3D scenarios is not easy due to the additional depth information in 3D data that triggers more complicated object arrangements and more complex descriptions to describe the relations between objects, leaving 3D visual grounding as an unsolved research area.

2.2 3D Visual Grounding

In 3D visual grounding, models are designed to jointly handle complicated natural language descriptions and scattered objects within a point cloud scene. Previous approaches attempt to solve this task by either constructing text-point-cloud feature alignment frameworks [21], designing pipelines to better exploit the 3D spatial relations of objects [2, 11, 15, 19, 44, 50], or bringing in auxiliary visual features [4, 20, 31, 46]. Specifically, BUTD-DETR [21] extends MDETR [23] to 3D visual grounding by adapting a text-point-cloud alignment loss to pull the features of point cloud and text together. To exploit the 3D spatial relations, graph-based methods [2, 15, 19, 50] utilize GNNs to model the 3D scene, with nodes and edges being the objects and object-to-object relations, to learn their correlations explicitly. Also, some studies craft specialized modules [11, 17, 40, 44], such as the spatial self-attention presented in ViL3DRel [11] and relation matching network in CORE-3DVG [44], to capture spatial relations among objects.

To better identify the target object of interest, some [4, 20, 31, 46] intend to produce richer input semantic information for the model. For example, [4, 31, 46] introduce image features by acquiring 2D images of the scene to obtain more color/shape information. On the other hand, MVT [20] projects the point cloud into multiple views for more position information. Although these approaches have achieved great progress in dealing with scattered object arrangements, such methods typically extract a global, sentence-level feature [13, 30] from the given natural description. As a result, detailed information within the description (*e.g.*, the target object, anchor objects, and their relations) may not be preserved and leveraged properly, potentially reducing training efficiency and prediction accuracy of the model as discussed in [5].

To address the above issue, some works have put their efforts into mining the natural descriptions to acquire additional prior knowledge for more efficient and effective learning [1, 5, 18, 42, 49]. Specifically, ScanEnts3d [1] and 3DPAG [49] recruit human annotators to establish one-to-one matching between each anchor object mentioned in the description and the corresponding object entity in the 3D scene. With this additional information, they design dense word-object alignment losses to improve the training. However, annotating one-to-one correlation requires considerable labor. For example, it takes 3664 hours of workforce commitment in 3DPAG to annotate anchor objects for 88k descriptions. To eliminate the need for human annotators, NS3D [18] makes the first attempt to use the

LLM. It leverages Codex [10] to parse fixed-template descriptions into nested logical expressions, followed by a neural-symbolic framework to execute the logical expressions implemented as programmatic functions.

Unfortunately, NS3D cannot handle arbitrary natural descriptions well, which might generate complicated expressions and unforeseen functions, hindering the framework from successful execution [18]. Recently, CoT3DRef [5] proposes to acquire the referential order of the description, listing from anchor objects to the final target object, using LLMs. Also, the authors design a rule-based searching method using a traditional sentence parser [37] to construct the one-to-one matching between class names in the order and potential anchor/target objects in the scene at once. The matching information is encoded by positional encoding as additional inputs for the proposed transformer-based CoT module to learn the referring process implicitly and predict the final target object. Nevertheless, since rule-based matching is not guaranteed to be correct, such additional inputs might result in noisy information and degrade the grounding process, impeding correct target prediction and affecting training stability.

3 Methodology

3.1 Problem Formulation and Framework Overview

Problem formulation We first define the setting and notations used in this paper. For each indoor scene, we have a set of colored point cloud $C \in \mathbb{R}^{N \times 6}$, where N denotes the number of the points in the scene, with each point represented in terms of its three-dimensional coordinate and RGB spaces. C is processed to acquire K object proposals $P = \{\mathbf{p}_1, \dots, \mathbf{p}_K\}$ that represent possible objects in the scene, with each proposal containing I points (*i.e.*, $\mathbf{p}_n \in \mathbb{R}^{I \times 6}$, $n \in [1, \dots, M]$). P is obtained either by pre-trained object segmentation networks [22, 34, 43] or directly from the dataset. Along with P , the class labels $L = \{l_1, \dots, l_K\}$ for all proposals are additionally predicted by a Pointnet++ [35] classifier. For 3D grounding, a text description D is given, illustrating the target object in C by describing its color, shape, or relations to other anchor objects. Given the above inputs, our goal is to identify the exact target object that matches D among all objects in the scene by predicting a K -dimensional confidence score $S = \{s_1, \dots, s_K\}$ for classifying the target object.

Framework overview As shown in Fig. 2, DOrA is composed of B consecutive Object-Referring blocks $\{R_1, \dots, R_B\}$ to progressively locate the target object. In particular, by taking both P and D as the inputs, DOrA utilizes the Object-Referring blocks $R_{1:B}$ in Fig. 2 to sequentially produce anchor objects to guide the grounding process. Each R_i takes the object feature $F_i \in \mathbb{R}^{K \times d_i}$ and the text feature $T \in \mathbb{R}^{(|D|+1) \times 768}$ as the inputs. Note that T contains a 1×768 -dimensional sentence-level feature and $|D| \times 768$ -dimensional word-level feature, where $|D|$ denotes the length of D after tokenization. By observing F_i and T , the

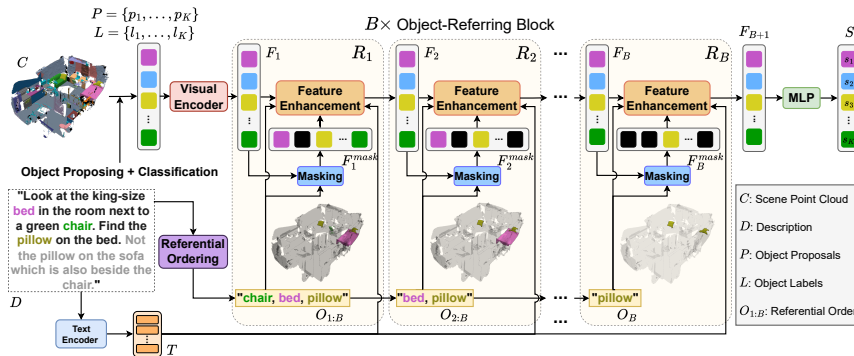


Fig. 2: Architecture of our 3D Visual Grounding Framework with Order-Aware Referring (DORa). By taking a point cloud scene C and a natural description D as inputs, our DORa produces a referential order of anchor objects $O_{1:B}$ and conduct Object-Referring blocks $R_{1:B}$ to locate the target object progressively.

Object-Referring block R_i aims to produce the refined feature F_{i+1} along with the updated anchor/target objects and their relations for grounding purposes.

To enable our Object-Referring blocks to capture proper information about the anchor/target objects, we apply a Large Language Model (LLM) to D to generate a Referential Order $O_{1:B} = \{O_1, \dots, O_B\}$ that mimics human perception system of searching target object [9, 32] by extracting and arranging the class names of the anchor and target objects. Specifically, $\{O_1, \dots, O_{B-1}\}$ represent the class names of the anchor objects, and O_B is the class name of the target object. Note that $O_{i:B}$ is observed by the i -th Object-Referring block R_i as guidance, which updates the features of anchor/target objects with the proposed Feature Enhancing (FE) module. Since there is no ground truth referential order of the produced anchor objects, we also introduce a pre-training strategy for training DORa. This is achieved by synthesizing *accurate* referential order and anchor/target object labels. With the above design, DORa can be applied for 3D grounding tasks and achieve satisfactory performances. We now detail the design of our DORa in the following subsections.

3.2 Referential Ordering using LLM

To have Object-Referring blocks $\{R_1, \dots, R_B\}$ to locate the target object properly, it is desirable to extract a proper referential order $O_{1:B}$ from the input description D . With such a referring path constructed, visual features of the associated objects can be updated for grounding purposes. This is inspired by the idea of Chain-of-Thoughts [26, 41] in LLM, as noted in CoT3DRef [5]. To achieve such a parsing task, we apply GPT-3.5-Turbo [48] as the description parser using in-context learning (ICL) [14], as depicted in Fig. 3a.

However, it is not trivial to have LLM output a referential order from D due to lengthy and noisy descriptions. For example, for an input description “Look at

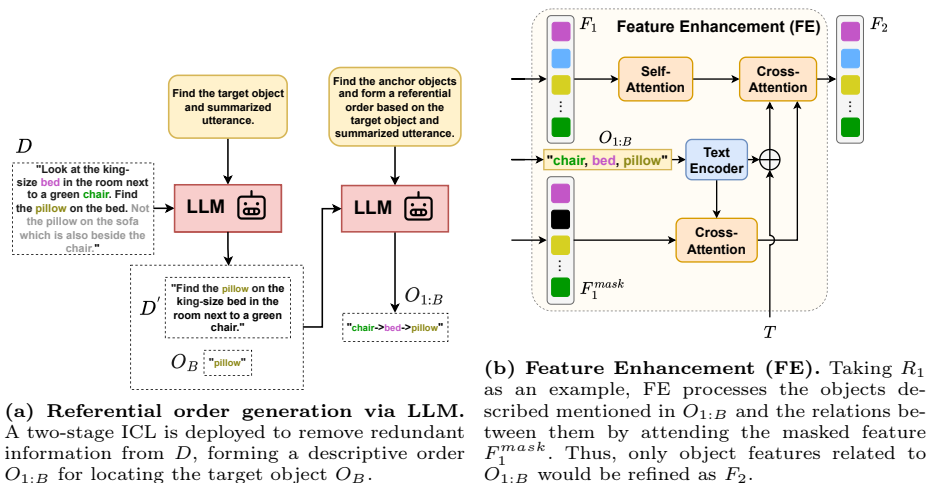


Fig. 3: Illustration of referential order generation and feature enhancement in DOrA.

the king-size bed in the room next to a green chair, Find the pillow on the bed. Not the pillow on the sofa which is also beside the chair.”, one would expect first to find the green *chair* then the king-size *bed* next to the chair, and finally, the *pillow* on the bed. Therefore, the ideal referential order is $\{\text{“chair”, “bed”, “pillow”}\}$. In the above example, the sentence “Not the pillow on the sofa which is also beside the chair.” is redundant since one can find the correct target object without this information. If we apply the LLM directly to the original description, the model may be misled by this redundant information and generate a referential order containing the object “sofa”.

To tackle the above problem, we conduct a two-stage in-context learning (ICL) scheme to remove redundant information in D before producing $O_{1:B}$, as depicted in Fig. 3a. With the given target object O_B , we predict a summarized description D' to remove redundant information in D in the first stage. Then, the entire referential order $O_{1:B}$ given D' and O_B is produced in the second stage. For each stage of our ICL, 10 examples are provided as demonstrations of the input prompts for LLM to predict $O_{1:B}$. Due to page limitations, demonstration examples and the complete prefix prompts are presented in the supplementary materials. With $O_{1:B}$ obtained, the order-aware object referring process can be processed accordingly, as we detail next.

3.3 3D Visual Grounding with Order-Aware Object Referring

Object-referring blocks. Given the object proposals P , the corresponding labels $L = \{l_1, \dots, l_K\}$, the encoded text features T , and the derived referential order $O_{1:B}$ the as inputs, our DOrA deploys a series of Object-Referring blocks $\{R_1, \dots, R_B\}$ to perform the grounding task. As depicted in Fig. 2, this referring process is conducted by leaving out an anchor object and updating the visual

features in each step, until only the final step locates the target object of interest. Thus, the deployment of Object-Referring blocks allows one to focus on the anchor/target objects, so that their visual features and spatial relations between them can be exploited with those of irrelevant objects disregarded.

Take the i -th referring block observing $O_{i:B}$ for example, a *masked feature* $F_i^{mask} = F_i \odot M_i$ is derived by applying a Hadamard product between F_i and a K -dimensional binary mask M_i to replace features of object proposals in F_i not belonging to any of the object classes in $O_{i:B}$. Such a masking strategy ensures that F_i^{mask} contains objects described in $O_{i:B}$ and hence explicitly suppresses effects of irrelevant objects that are not in our interests. Thus, the j -th entry of M_i (denoted as m_{ij}) is defined as:

$$m_{ij} = \begin{cases} 1 & \text{if class name of } l_j \text{ is in } O_{i:B}, \\ 0 & \text{otherwise.} \end{cases} \quad (1)$$

F_i and F_i^{mask} are refined into F_{i+1} for the next referring block via the feature enhancement module (as discussed later). At the final stage, the output F_{B+1} of R_B is utilized to predict the confidence score S that represents the identity of the target object, supervised by a cross-entropy loss \mathcal{L}_{ref} . Additionally, to ensure the text feature T properly describing the anchor/target objects, we follow CoT3DRef [5] and apply the language classification loss \mathcal{L}_{text} to T for matching the associated class labels.

Object feature enhancement. With the above masking process, each object-referring block is expected to update the object features related to the anchor and target objects. This is realized by our attention-based Feature Enhancement (FE) module. To be more precise, in order to update the features associated with the anchor and target objects in R_i according to F_i , F_i^{mask} , T and $O_{i:B}$, our FE module aims to exploit their visual features and spatial relations through attention mechanisms.

Take the FE module in R_1 as an example, as depicted in Fig. 3b, we start with the lower branch which locally emphasizes the features of the potential anchor/target objects via a cross-attention layer by treating F_i^{mask} as value/key and encoded text feature of $O_{1:B}$ (denoted as $T_{O_{1:B}}$) as query. On the other hand, the upper branch of Fig. 3b explores the spatial relations between all objects by treating the self-attended F_1 as key/value of another cross-attention, with the concatenation of $T_{O_{1:B}}$ and T being query. Finally, an additional cross-attention layer is applied to the previous output features of both branches to obtain the enhanced proposal feature F_2 , which enriches not only the information of anchor/target objects but also the relations between them.

On the other hand, to prevent the information extracted from the anchor/target objects from vanishing (i.e., F_2 becomes identical to F_1) during FE, we introduce an additional masking loss \mathcal{L}_{mask} by projecting F_2 from $K \times d_2$ -dimensional to $K \times 1$ -dimensional digits with MLPs to classify if each proposal in F_2 is previ-

ously masked in F_1^{mask} . The masking loss \mathcal{L}_{mask} is defined as:

$$\mathcal{L}_{mask} = \mathcal{L}_{BCE}(MLP(F_2), M_1), \quad (2)$$

where M_1 represents the K -dimensional binary mask as defined in Eq. (1). It is worth noting that, \mathcal{L}_{mask} is applied to output features of each referring block with a similar formulation to ensure each output feature contains the information of the current anchor/target objects correspondingly.

3.4 Order-Aware Pre-training with Synthetic Referential Order

Although DOrA is designed to produce a referential order of anchor objects for localizing the target object, only the ground truth point cloud information of the target object is given during training. Thus, the above framework is viewed as a weakly-supervised learning scheme since there is *no* ground truth referential order available during training. To provide better training supervision, we pre-train DOrA with a simple yet proper synthetic 3D visual grounding task, where the ground-truth labels of anchor/target objects and descriptions with accurate referential orders can be obtained. This pre-training strategy is presented below.

Augmenting plausible referential order and description To provide better training supervision and to ensure the reliability of our synthesized data, the constructed description and the corresponding referential order need to be easily and uniquely determined based on anchor/target objects. In our work, we choose to consider spatial relations between objects that are independent of viewpoint (e.g., “*nearest*” or “*farthest*”) as the constructing descriptions, suggesting the referential order of anchor/target objects during this data augmentation stage. As highlighted in Algorithm A1 of our supplementary material, given P , L , and B , we construct an augmented referential order $O_{1:B}^{aug}$ by choosing B different class labels $\{l_1^{aug}, \dots, l_B^{aug}\}$ from L and extracting their class names. The augmented description D^{aug} is then derived as:

“There is a $\{O_1^{aug}\}$ in the room, find the $\{O_2^{aug}\}$ farthest to it, and then find the $\{O_3^{aug}\}$ farthest to that $\{O_2^{aug}\}$, $\{...\}$, finally you can see the $\{O_B^{aug}\}$ farthest to that $\{O_{B-1}^{aug}\}$.”

Since D^{aug} is constructed following the appearing sequence of object names in $O_{1:B}^{aug}$, it is guaranteed that $O_{1:B}^{aug}$ is a correct referential order w.r.t. D^{aug} and thus can be served as ground truth supervision for pre-training DOrA.

It is worth noting that, to have each object in D^{aug} uniquely defined, we only keep one proposal p_1^{aug} with the class name of $\{O_1^{aug}\}$ in P and remove all the other proposals with that class name. As a result, all the anchor and target objects in P (denoted as $p_{1:B}^{aug} = \{p_1^{aug}, \dots, p_B^{aug}\}$) according to D^{aug} and their corresponding identities are uniquely determined (i.e., p_2^{aug} is assigned by finding the farthest proposal against p_1^{aug} with label l_2^{aug} , and the rest of the anchor/target objects are determined consecutively with the same strategy).

Pre-training objectives To have DOrA follow $O_{1:B}^{aug}$ to refer p_i^{aug} in the i -th referring block R_i , we design a coordinate loss \mathcal{L}_{crd} to encourage the output feature F_{i+1} of R_i to identify the coordinate of all proposals in P w.r.t. p_i^{aug} . Thus, we calculate \mathcal{L}_{crd} as:

$$\mathcal{L}_{crd} = \frac{1}{B} \sum_{i=1}^B \mathcal{L}_{MSE}(MLP(F_{i+1}), V - \mathbb{I} \cdot v_i), \quad (3)$$

where $MLP(\cdot)$ represents MLP layers applied to F_{i+1} , V is a $K \times 3$ matrix representing center coordinates of calculated bounding-boxes of all K proposals in P , \mathbb{I} stands for a $K \times 1$ -dimensional identity vector, and v_i is the 1×3 -dimensional center coordinate of p_i^{aug} .

We note that, the referential loss \mathcal{L}_{ref} mentioned in Sec. 3.3 is also extended to classify both the identity of anchor objects using $F_{2:B}$ and the identity of the target object for F_{B+1} during the pre-training. To this end, we can define the objectives used during our pre-training by summing up the referential loss \mathcal{L}_{ref} (for both anchor and target objects), the masking loss \mathcal{L}_{mask} , the language classification loss \mathcal{L}_{text} and the coordinate loss \mathcal{L}_{crd} .

3.5 Overall Training Pipeline

We now summarize the training of DOrA. With the pre-training stage noted in Sec. 3.4 to warm up the model, we take point cloud data with real-world natural descriptions to continue the training process. Since the identity of anchor objects is unknown, we only apply \mathcal{L}_{ref} (for the target object only), \mathcal{L}_{mask} , and \mathcal{L}_{text} as supervision. The overall training pipeline is summarized in Algorithm A2 of our supplementary material.

4 Experiments

4.1 Datasets

NR3D NR3D [2] dataset consists of 707 indoor scenes in ScanNet [12] with 28715/7485 description-target pairs in the training/testing set, where the descriptions are collected from human annotators. There are 524 different object classes in the scenes in total. NR3D assumes perfect class-agnostic object proposals, where each point in the scene is properly assigned to its corresponding proposal. As a result, models are only required to classify the target object that uniquely matches the description among all proposals in the scene, with classification accuracy (Acc in %) being the metric. Please refer to the supplementary material for the details of the implementation.

ScanRefer ScanRefer [8] contains 36665/9508 description-target pairs across a total of 800 indoor scenes in its training/validation set, where the descriptions are also collected from human annotators. Also derived from ScanNet [12] but

Table 1: Grounding accuracy (%) on NR3D. Note that each column shows the results trained with a specific amount of training data.

Method	Labeled Training Data				
	1%	2.5%	5%	10%	100%
Referit3D [2]	4.4	13.6	20.3	23.3	35.6
TransRefer3D [17]	11.0	16.1	21.9	25.7	42.1
SAT [46]	11.6	16.0	21.4	25.0	49.2
BUTD-DETR [21]	<u>24.2</u>	<u>28.6</u>	<u>31.2</u>	33.3	54.6
MVT [20]	9.9	16.1	21.6	26.5	55.1
MVT [20] + CoT3DRef [5]	-	-	-	<u>38.2</u>	60.4
DOrA (Ours)	33.5	36.1	41.5	46.0	<u>59.7</u>

different from NR3D, perfect object proposals are not available in ScanRefer, and therefore additional object proposers are required for all methods. Nevertheless, Acc in % under 0.25 and 0.5 intersection over union (IoU) are used as the metrics for ScanRefer. Please refer to the supplementary material for the details of the implementation.

4.2 Quantitative Results

We present the quantitative results on NR3D and ScanRefer, with consideration of different amounts of available training samples against several baselines by reproducing from their official implementation. As shown in Tab. 1, DOrA possesses a considerably superior performance when training with 1% (287), 2.5% (717), 5% (1435), and 10% (2871) NR3D training set samples. Specifically, using only 10% data, DOrA achieves 46.0 overall Acc, which outperforms Referit3D and TransRefer3D with 100% (28715) data. When training with 100% data, DOrA achieves comparable results to MVT augmented with CoT3DRef³, which requires additional prior linguistic knowledge about the dataset for its rule-based algorithm to construct a one-to-one relation between each anchor’s class name and corresponding object identity.

Tab. 2 further displays the detailed performance on different official subsets of NR3D. Among the subsets, the **Hard** subset contains samples with more than 2 distractors, where a distractor is an object having the same class name as the target object, and the **Easy** subset is the contrary. **View-dependent** samples contain relations where rotating the point cloud scene will affect the referred ground-truth target object (e.g., left and right), and **View-independent** samples are contrary. DOrA accentuates itself with decent capabilities on different subsets, consistently followed by BUTD-DETR [21] that also features a self-designed DETR-based data augmentation for 3D visual grounding.

Finally, Tab. 3 presents DOrA’s performance on ScanRefer, where ground-truth object proposals are unavailable. We can see that our DOrA demonstrates

³ Performance of MVT+CoT3DRef on 1%, 2.5%, and 5% training data are not available since its referential order and 1-to-1 class-identity relation are not publicly available. Only their results of 10% and 100% data are presented.

Table 2: Grounding accuracy on the official NR3D subsets [2]. For implementation and comparison purposes, only the setting of 10% of training data is considered.

Method	Hard	Easy	View-Dep.	View-Indep.	Overall
Referit3D [2]	19.5	27.3	21.2	24.2	23.3
TransRefer3D [17]	21.6	29.9	22.9	27.0	25.7
SAT [46]	22.5	27.6	21.7	26.6	25.0
BUTD-DETR [21]	<u>25.9</u>	<u>41.9</u>	<u>29.1</u>	<u>34.8</u>	<u>33.3</u>
MVT [20]	22.9	30.3	25.4	27.1	26.5
DOrA (Ours)	39.1	53.3	45.3	46.4	46.0

Table 3: Grounding accuracy (%) on the ScanRefer validation set. Note that different amounts of training data are considered.

Method	Labeled Training Data					
	5%		10%		100%	
	Acc@0.25	Acc@0.5	Acc@0.25	Acc@0.5	Acc@0.25	Acc@0.5
ScanRefer [8]	23.0	12.0	27.4	15.0	35.5	22.4
3DVG-Trans. [53]	35.3	23.3	39.0	29.0	45.9	34.5
3D-SPS [31]	28.4	16.9	32.9	22.9	48.8	37.0
BUTD-DETR [21]	<u>38.2</u>	26.2	<u>40.3</u>	28.3	52.2	39.8
M3DRef-CLIP [52]	37.2	<u>29.9</u>	40.0	<u>32.4</u>	52.5	<u>44.7</u>
CORE-3DVG [44]	-	-	-	-	56.8	43.8
DOrA (Ours)	39.8	31.5	43.6	34.9	<u>52.8</u>	44.8

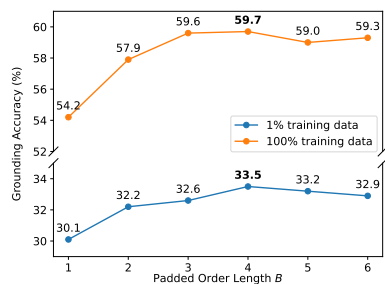
slightly preferable results with only 5% and 10% of data compared to other approaches. It is comparable to SOTA methods when given 100% data. Note that we only report CORE-3DVG’s [44] results on 100% (36665) ScanRefer training samples since its implementation is currently unavailable.

4.3 Ablation Studies

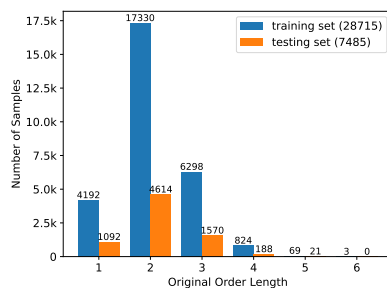
Component analysis We ablate different components of our DOrA in Tab. 4, with performances under **1%** and **100%** training samples available. Baseline model A extracts class names of anchor/target objects from D using a language parser [6] and constructs the referential order according to the appearance of the names in D directly. Also, we employ each of our Referring Blocks R_i in model A without the FE module, *i.e.*, directly using F_i to calculate attention with text features of $O_{i:B}$ and D . Model B enhances the accuracy on 1% training data by conducting our two-stage object ordering with LLM. When further applying the order-aware pre-training in model C, significant improvements in both settings, especially for 1% available data, are observed. The scarcity of training data often impedes the ability of the model to learn the concept of order and relations among objects implicitly. By conducting our pre-training strategy, our DOrA is able to learn foundational concepts of ordering and relations to locate the target objects progressively. Finally, our full model in the last row, incorporating FE modules each R_i to enhance features of anchor/target objects with F_i^{mask} ,

Table 4: Ablation studies of proposed components in DOrA. For methods without LLM Object Ordering, we form $O_{1:B}$ according to the appearance of anchor/target object names in D . Both cases of 1% and 100% training data are considered.

	FE Module	Order-Aware Pre-training	LLM Object Ordering	1%	100%
A				8.9	53.9
B			✓	10.3	53.8
C		✓	✓	25.8	58.0
Ours	✓	✓	✓	33.5	59.7



(a) Grounding accuracies with different maximum (padded) referential order length B . Note that B is equal to and denoted as the number of Object-Referring blocks.



(b) Statistics of the referential order length in NR3D. A longer referential order denotes a more complex referring process for grounding.

Fig. 4: (a) Grounding accuracies with varying Object-Referring block numbers B and (b) statistics of referential order length of NR3D. It can be seen that the model performance saturates at $B=4$, matching length statistics of NR3D.

achieves optimal results on both settings. This verifies the success of our proposed modules and pre-training strategy.

Length of referential order We additionally analyze the effectiveness of padded order length B of $O_{1:B}$ (and also the number of Referring Blocks) in 4, which illustrates the performances with different B using 1% and 100% training data in Fig. 4a. We also show the statistics of the original order length generated by our two-stage referential ordering in Fig. 4b. We observe that although performances gradually increase with larger B (*i.e.*, considering more potential anchor objects appeared in D achieves better accuracy), the performance gain saturates at $B = 4$. This can be explained by looking at Fig. 4b, which shows that only a very few amount of data exceeds an order length of 4 in both training and testing pairs. This suggests that our selection of $B = 4$ is reasonable, optimally balancing computational efficiency with prediction accuracy.

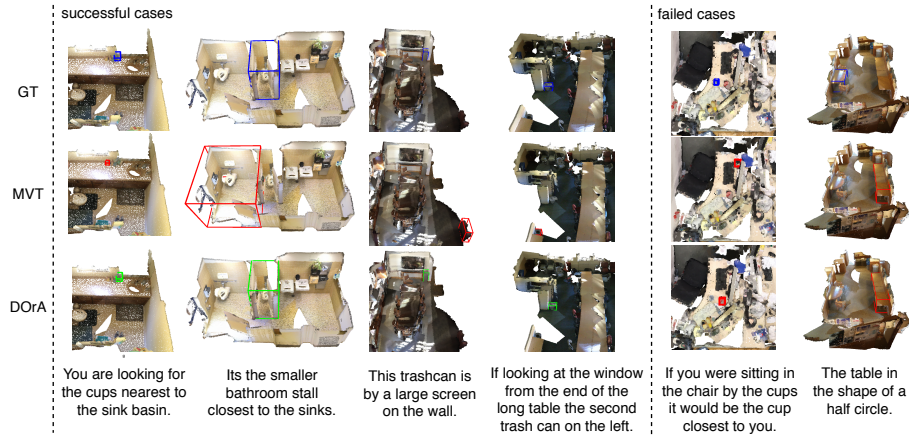


Fig. 5: 3D grounding examples of NR3D. Note that blue/green/red boxes denote ground truth/correct/incorrect predictions. While both MVT and DOrA fail on the last two cases, it is due to the fact that the size of the target object is extremely small (e.g., cup) and the description does *not* describe any anchor objects.

4.4 Qualitative Results

Fig. 5 demonstrates the qualitative results of DOrA on NR3D, with MVT being the baseline. We display four successful cases and two failed cases. It is shown that DOrA can successfully identify the target object referred by one to multiple anchor objects, even in lengthy descriptions. Failed cases include those that refer by shapes or have a very small target object that is hard for Pointnet++ to capture visual information.

5 Conclusions and Limitations

Conclusions We presented a 3D visual grounding framework with **Order-Aware** referring (DOrA) in this paper. DOrA leverages LLM to identify anchor/target objects from the input description as a referential order, guiding the updates of the associated object features for grounding purposes. The above process is realized by stacked Object-Referring blocks in DOrA, which progressively refine the features for the objects of interest in the referential order. In addition, we also designed a pre-training scheme which augments a pseudo yet correct series of anchor/target objects for warming up DOrA in a supervised fashion. Experiments on benchmark datasets demonstrate that our DOrA performed favorably against SOTA 3D grounding works across different settings.

Limitations Since DOrA utilizes LLMs to generate the referential order from the input description, despite of our introduced pre-training strategy to warm the training process, the correctness of the extracted referential order would affect the training and the performance of DOrA.

References

1. Abdelreheem, A., Olszewski, K., Lee, H.Y., Wonka, P., Achlioptas, P.: Scanents3d: Exploiting phrase-to-3d-object correspondences for improved visio-linguistic models in 3d scenes. In: Proceedings of the IEEE/CVF Winter Conference on Applications of Computer Vision (WACV). pp. 3524–3534 (2024) [2](#), [4](#)
2. Achlioptas, P., Abdelreheem, A., Xia, F., Elhoseiny, M., Guibas, L.: Referit3d: Neural listeners for fine-grained 3d object identification in real-world scenes. In: Proceedings of the European Conference on Computer Vision (ECCV). pp. 422–440. Springer (2020) [2](#), [4](#), [10](#), [11](#), [12](#), [20](#)
3. Anderson, P., Wu, Q., Teney, D., Bruce, J., Johnson, M., Sünderhauf, N., Reid, I., Gould, S., Van Den Hengel, A.: Vision-and-language navigation: Interpreting visually-grounded navigation instructions in real environments. In: Proceedings of the IEEE conference on computer vision and pattern recognition (CVPR). pp. 3674–3683 (2018) [2](#)
4. Bakr, E., Alsaedy, Y., Elhoseiny, M.: Look around and refer: 2d synthetic semantics knowledge distillation for 3d visual grounding. In: Proceedings of Advances in Neural Information Processing Systems (NeurIPS). vol. 35 (2022) [2](#), [4](#)
5. Bakr, E.M., Ayman, M., Ahmed, M., Slim, H., Elhoseiny, M.: Cot3dref: Chain-of-thoughts data-efficient 3d visual grounding. arXiv preprint arXiv:2310.06214 (2023) [2](#), [4](#), [5](#), [6](#), [8](#), [11](#), [20](#), [21](#), [24](#), [25](#)
6. Bird, S., Klein, E., Loper, E.: Natural language processing with Python: analyzing text with the natural language toolkit. " O'Reilly Media, Inc." (2009) [12](#)
7. Carion, N., Massa, F., Synnaeve, G., Usunier, N., Kirillov, A., Zagoruyko, S.: End-to-end object detection with transformers. In: Proceedings of the European conference on computer vision (ECCV). pp. 213–229. Springer (2020) [3](#)
8. Chen, D.Z., Chang, A.X., Nießner, M.: Scanrefer: 3d object localization in rgb-d scans using natural language. In: Proceedings of the European conference on computer vision (ECCV). pp. 202–221. Springer (2020) [2](#), [10](#), [12](#), [20](#)
9. Chen, L., Lambon Ralph, M.A., Rogers, T.T.: A unified model of human semantic knowledge and its disorders. Nature human behaviour p. 0039 (2017) [2](#), [6](#)
10. Chen, M., Tworek, J., Jun, H., Yuan, Q., Pinto, H.P.d.O., Kaplan, J., Edwards, H., Burda, Y., Joseph, N., Brockman, G., et al.: Evaluating large language models trained on code. arXiv preprint arXiv:2107.03374 (2021) [2](#), [5](#)
11. Chen, S., Guhur, P.L., Tapaswi, M., Schmid, C., Laptev, I.: Language conditioned spatial relation reasoning for 3d object grounding. In: Proceedings of Advances in Neural Information Processing Systems (NeurIPS). vol. 35 (2022) [2](#), [4](#)
12. Dai, A., Chang, A.X., Savva, M., Halber, M., Funkhouser, T., Nießner, M.: Scannet: Richly-annotated 3d reconstructions of indoor scenes. In: Proceedings of the IEEE conference on computer vision and pattern recognition (CVPR). pp. 5828–5839 (2017) [2](#), [10](#)
13. Devlin, J., Chang, M.W., Lee, K., Toutanova, K.: BERT: Pre-training of deep bidirectional transformers for language understanding. In: Proceedings of the Conference of the North American Chapter of the Association for Computational Linguistics (NAACL). pp. 4171–4186 (2019) [4](#), [20](#)
14. Dong, Q., Li, L., Dai, D., Zheng, C., Wu, Z., Chang, B., Sun, X., Xu, J., Sui, Z.: A survey for in-context learning. arXiv preprint arXiv:2301.00234 (2022) [6](#)
15. Feng, M., Li, Z., Li, Q., Zhang, L., Zhang, X., Zhu, G., Zhang, H., Wang, Y., Mian, A.: Free-form description guided 3d visual graph network for object grounding in point cloud. In: Proceedings of the IEEE/CVF International Conference on Computer Vision (ICCV). pp. 3722–3731 (2021) [2](#), [4](#)

16. Hao, Z., Feng, L., Shilong, L., Lei, Z., Hang, S., Jun, Z., Ni, L.M., Heung-Yeung, S.: DINO: DETR with improved denoising anchor boxes for end-to-end object detection. In: Proceedings of the International Conference on Learning Representations (ICLR) (2023) [4](#)
17. He, D., Zhao, Y., Luo, J., Hui, T., Huang, S., Zhang, A., Liu, S.: Transrefer3d: Entity-and-relation aware transformer for fine-grained 3d visual grounding. In: Proceedings of the 29th ACM International Conference on Multimedia (MM). pp. 2344–2352 (2021) [2](#), [4](#), [11](#), [12](#), [20](#)
18. Hsu, J., Mao, J., Wu, J.: Ns3d: Neuro-symbolic grounding of 3d objects and relations. In: Proceedings of the IEEE/CVF Conference on Computer Vision and Pattern Recognition (CVPR). pp. 2614–2623 (2023) [2](#), [4](#), [5](#)
19. Huang, P.H., Lee, H.H., Chen, H.T., Liu, T.L.: Text-guided graph neural networks for referring 3d instance segmentation. In: Proceedings of the AAAI Conference on Artificial Intelligence. pp. 1610–1618 (2021) [2](#), [4](#)
20. Huang, S., Chen, Y., Jia, J., Wang, L.: Multi-view transformer for 3d visual grounding. In: Proceedings of the IEEE/CVF Conference on Computer Vision and Pattern Recognition (CVPR). pp. 15524–15533 (2022) [2](#), [4](#), [11](#), [12](#), [20](#), [25](#), [26](#)
21. Jain, A., Gkanatsios, N., Mediratta, I., Fragkiadaki, K.: Bottom up top down detection transformers for language grounding in images and point clouds. In: Proceedings of the European Conference on Computer Vision (ECCV). pp. 417–433. Springer (2022) [2](#), [4](#), [11](#), [12](#), [20](#)
22. Jiang, L., Zhao, H., Shi, S., Liu, S., Fu, C.W., Jia, J.: Pointgroup: Dual-set point grouping for 3d instance segmentation. In: Proceedings of the IEEE/CVF Conference on Computer Vision and Pattern Recognition (CVPR). pp. 4867–4876 (2020) [5](#), [20](#)
23. Kamath, A., Singh, M., LeCun, Y., Synnaeve, G., Misra, I., Carion, N.: Mdetr-modulated detection for end-to-end multi-modal understanding. In: Proceedings of the IEEE/CVF International Conference on Computer Vision (ICCV). pp. 1780–1790 (2021) [2](#), [3](#), [4](#)
24. Kingma, D.P., Jimmy, B.: Adam: A method for stochastic optimization. In: Proceedings of the International Conference on Learning Representations (ICLR) (2015) [19](#)
25. Kochanski, R.B., Lombardi, J.M., Laratta, J.L., Lehman, R.A., O’Toole, J.E.: Image-guided navigation and robotics in spine surgery. *Neurosurgery* pp. 1179–1189 (2019) [2](#)
26. Kojima, T., Gu, S.S., Reid, M., Matsuo, Y., Iwasawa, Y.: Large language models are zero-shot reasoners. In: Proceedings of Advances in Neural Information Processing Systems (NeurIPS). vol. 35 (2022) [6](#)
27. Lee, L.H., Braud, T., Zhou, P., Wang, L., Xu, D., Lin, Z., Kumar, A., Bermejo, C., Hui, P.: All one needs to know about metaverse: A complete survey on technological singularity, virtual ecosystem, and research agenda. arXiv preprint arXiv:2110.05352 (2021) [2](#)
28. Li, L.H., Zhang, P., Zhang, H., Yang, J., Li, C., Zhong, Y., Wang, L., Yuan, L., Zhang, L., Hwang, J.N., et al.: Grounded language-image pre-training. In: Proceedings of the IEEE/CVF Conference on Computer Vision and Pattern Recognition (CVPR). pp. 10965–10975 (2022) [3](#)
29. Liu, S., Zeng, Z., Ren, T., Li, F., Zhang, H., Yang, J., Li, C., Yang, J., Su, H., Zhu, J., et al.: Grounding dino: Marrying dino with grounded pre-training for open-set object detection. arXiv preprint arXiv:2303.05499 (2023) [2](#), [3](#), [4](#)

30. Liu, Y., Ott, M., Goyal, N., Du, J., Joshi, M., Chen, D., Levy, O., Lewis, M., Zettlemoyer, L., Stoyanov, V.: Roberta: A robustly optimized bert pretraining approach. arXiv preprint arXiv:1907.11692 (2019) [4](#)
31. Luo, J., Fu, J., Kong, X., Gao, C., Ren, H., Shen, H., Xia, H., Liu, S.: 3d-sps: Single-stage 3d visual grounding via referred point progressive selection. In: Proceedings of the IEEE/CVF Conference on Computer Vision and Pattern Recognition (CVPR). pp. 16454–16463 (2022) [2](#), [4](#), [12](#), [20](#)
32. McVay, J.C., Kane, M.J.: Conducting the train of thought: working memory capacity, goal neglect, and mind wandering in an executive-control task. *Journal of Experimental Psychology: Learning, Memory, and Cognition* p. 196 (2009) [2](#), [6](#)
33. Paszke, A., Gross, S., Massa, F., Lerer, A., Bradbury, J., Chanan, G., Killeen, T., Lin, Z., Gimelshein, N., Antiga, L., et al.: Pytorch: An imperative style, high-performance deep learning library. In: Proceedings of Advances in Neural Information Processing Systems (NeurIPS). vol. 32 (2019) [19](#)
34. Qi, C.R., Litany, O., He, K., Guibas, L.J.: Deep hough voting for 3d object detection in point clouds. In: Proceedings of the IEEE/CVF International Conference on Computer Vision (ICCV). pp. 9277–9286 (2019) [5](#)
35. Qi, C.R., Yi, L., Su, H., Guibas, L.J.: Pointnet++: Deep hierarchical feature learning on point sets in a metric space. In: Proceedings of Advances in neural information processing systems (NeurIPS). vol. 30 (2017) [5](#), [20](#)
36. Scarselli, F., Gori, M., Tsoi, A.C., Hagenbuchner, M., Monfardini, G.: The graph neural network model. *IEEE Transactions on Neural Networks* pp. 61–80 (2008) [2](#)
37. Schuster, S., Krishna, R., Chang, A., Fei-Fei, L., Manning, C.D.: Generating semantically precise scene graphs from textual descriptions for improved image retrieval. In: Proceedings of the fourth workshop on vision and language. pp. 70–80 (2015) [5](#)
38. Shtedritski, A., Rupprecht, C., Vedaldi, A.: What does clip know about a red circle? visual prompt engineering for vlms. In: Proceedings of the IEEE/CVF International Conference on Computer Vision (ICCV). pp. 11987–11997 (2023) [2](#), [3](#)
39. Subramanian, S., Merrill, W., Darrell, T., Gardner, M., Singh, S., Rohrbach, A.: Reclip: A strong zero-shot baseline for referring expression comprehension. In: Proceedings of the Annual Meeting of the Association for Computational Linguistics (ACL) (2022) [3](#)
40. Wang, Z., Huang, H., Zhao, Y., Li, L., Cheng, X., Zhu, Y., Yin, A., Zhao, Z.: 3DRP-net: 3D relative position-aware network for 3D visual grounding. In: Proceedings of the 2023 Conference on Empirical Methods in Natural Language Processing (EMNLP) (2023) [2](#), [4](#)
41. Wei, J., Wang, X., Schuurmans, D., Bosma, M., Xia, F., Chi, E., Le, Q.V., Zhou, D., et al.: Chain-of-thought prompting elicits reasoning in large language models. In: Proceedings of Advances in Neural Information Processing Systems (NeurIPS). vol. 35 (2022) [6](#)
42. Wu, Y., Cheng, X., Zhang, R., Cheng, Z., Zhang, J.: Eda: Explicit text-decoupling and dense alignment for 3d visual grounding. In: Proceedings of the IEEE/CVF Conference on Computer Vision and Pattern Recognition (CVPR). pp. 19231–19242 (2023) [2](#), [4](#)
43. Wu, Y., Shi, M., Du, S., Lu, H., Cao, Z., Zhong, W.: 3d instances as 1d kernels. In: Proceedings of the European Conference on Computer Vision (ECCV). pp. 235–252. Springer (2022) [5](#)

44. Yang, L., Zhang, Z., Qi, Z., Xu, Y., Liu, W., Shan, Y., Li, B., Yang, W., Li, P., Wang, Y., et al.: Exploiting contextual objects and relations for 3d visual grounding. In: Proceedings of Advances in Neural Information Processing Systems (NeurIPS). vol. 36 (2024) [4](#), [12](#), [20](#), [21](#)
45. Yang, L., Wang, Y., Li, X., Wang, X., Yang, J.: Fine-grained visual prompting. In: Proceedings of Advances in Neural Information Processing Systems (2024) [2](#), [3](#)
46. Yang, Z., Zhang, S., Wang, L., Luo, J.: Sat: 2d semantics assisted training for 3d visual grounding. In: Proceedings of the IEEE/CVF International Conference on Computer Vision (ICCV). pp. 1856–1866 (2021) [2](#), [4](#), [11](#), [12](#), [20](#)
47. Yao, Y., Zhang, A., Zhang, Z., Liu, Z., Chua, T.S., Sun, M.: Cpt: Colorful prompt tuning for pre-trained vision-language models. arXiv preprint arXiv:2109.11797 (2021) [3](#)
48. Ye, J., Chen, X., Xu, N., Zu, C., Shao, Z., Liu, S., Cui, Y., Zhou, Z., Gong, C., Shen, Y., et al.: A comprehensive capability analysis of gpt-3 and gpt-3.5 series models. arXiv preprint arXiv:2303.10420 (2023) [3](#), [6](#), [21](#)
49. Yuan, Z., Yan, X., Li, Z., Li, X., Guo, Y., Cui, S., Li, Z.: Toward explainable and fine-grained 3d grounding through referring textual phrases. arXiv preprint arXiv:2207.01821 (2022) [2](#), [4](#)
50. Yuan, Z., Yan, X., Liao, Y., Zhang, R., Wang, S., Li, Z., Cui, S.: Instancerefer: Cooperative holistic understanding for visual grounding on point clouds through instance multi-level contextual referring. In: Proceedings of the IEEE/CVF International Conference on Computer Vision (ICCV). pp. 1791–1800 (2021) [4](#)
51. Zhang, H., Zhang, P., Hu, X., Chen, Y.C., Li, L., Dai, X., Wang, L., Yuan, L., Hwang, J.N., Gao, J.: Glipv2: Unifying localization and vision-language understanding. In: Proceedings of Advances in Neural Information Processing Systems (NeurIPS). vol. 35 (2022) [2](#), [3](#)
52. Zhang, Y., Gong, Z., Chang, A.X.: Multi3drefer: Grounding text description to multiple 3d objects. In: Proceedings of the IEEE/CVF International Conference on Computer Vision (CVPR). pp. 15225–15236 (2023) [12](#), [20](#)
53. Zhao, L., Cai, D., Sheng, L., Xu, D.: 3dvg-transformer: Relation modeling for visual grounding on point clouds. In: Proceedings of the IEEE/CVF International Conference on Computer Vision (ICCV). pp. 2928–2937 (2021) [12](#), [20](#)
54. Zhao, Y., Lin, Z., Zhou, D., Huang, Z., Feng, J., Kang, B.: Bubogpt: Enabling visual grounding in multi-modal llms. arXiv preprint arXiv:2307.08581 (2023) [2](#)

A More Details of DOrA

This section provides more details regarding model implementations and experimental setups. In particular, we first demonstrate the pseudocode of order-aware sample synthesis for pre-training in Sec. 3.4 and the complete training pipeline in Sec. 3.5. Then, we elaborate on the hyperparameters of DOrA and implementations of baselines for experiments in Sec. 4.

A.1 Pre-Training Sample Synthesis and Training Pipeline

This section provides the pseudocode of synthesizing order-aware samples for DOrA’s pre-training in Sec. 3.4 and the complete training pipeline in Sec. 3.5 in our main paper, respectively. Specifically, the Algorithm A1 demonstrates the pipeline to synthesize an order-aware pre-training sample given simply object proposals P and predicted object labels L . On the other hand, Algorithm A2 illustrates the complete pipeline to train DOrA with synthesized samples and natural-description samples, such as NR3D and ScanRefer.

Algorithm A1 Order-Aware Sample synthesis for DOrA Pre-training

Input: P and L
Hyperparameters: B
Output: D^{aug} , $O_{1:B}^{aug}$, and $p_{1:B}^{aug}$

- 1: randomly sample and arrange $\{l_1^{aug}, \dots, l_B^{aug}\}$ from L .
- 2: extract class names of $\{l_1^{aug}, \dots, l_B^{aug}\}$ as $O_{1:B}^{aug} = \{O_1^{aug}, \dots, O_B^{aug}\}$.
- 3: $D^{aug} =$ “There is a $\{O_1^{aug}\}$ in the room, find the $\{O_2^{aug}\}$ farthest to it, and then find the $\{O_3^{aug}\}$ farthest to that $\{O_2^{aug}\}$, $\{\dots\}$, finally you can see the $\{O_B^{aug}\}$ farthest to that $\{O_{B-1}^{aug}\}$.”
- 4: get p_1^{aug} by randomly removing objects in P with class of O_1^{aug} until only one of them is left.
- 5: initialize the anchor/target objects set as $\{p_1^{aug}\}$.
- 6: **for** $i = 2, 3, \dots, B$ **do**
- 7: for all objects in P with the class of O_i^{aug} , find the one farthest from p_{i-1}^{aug} to be p_i^{aug} .
- 8: append p_i^{aug} to $\{p_1^{aug}, \dots, p_{i-1}^{aug}\}$.
- 9: **end for**
- 10: $p_{1:B}^{aug} \leftarrow \{p_1^{aug}, \dots, p_B^{aug}\}$
- 11: **return** D^{aug} , $O_{1:B}^{aug}$, and $p_{1:B}^{aug}$

A.2 Implementation and Details and Experimental Settings

For both datasets, we use PyTorch [33] library to implement DOrA. We train DOrA using Adam [24] optimizer with a single NVIDIA Tesla V100 GPU. To conduct batch-wise training with a fixed number of Object-Referring blocks, we

set the length of referential order B to be 4, *i.e.*, we trim the original referential order from the front if its length exceeds 4 and pad it if its length is lower than 4. We adopt BERT [13] as the text encoder to extract T and Pointnet++ [35] as the visual encoder to acquire F_1 . We sample $I=1024$ points for each object proposal in the scene. Object proposal number K and token number $|D|$ are sample-dependent. Object feature dimension d_i for i -th Object-Referring block is set to 768, aligning with BERT’s 768 dimension, to conduct cross-attention.

Algorithm A2 DOrA Training Pipeline

Input: scene-description paired training samples $\{\{C_1, D_1\}, \{C_2, D_2\}, \dots\}$

Hyperparameters: pre-training step S_p , official training step S_o , and B

- 1: initialize DOrA’s model weights ϕ .
 - 2: $L_{pre} \leftarrow \{\mathcal{L}_{text}, \mathcal{L}_{mask}, \mathcal{L}_{ref}, \mathcal{L}_{crd}\}$
 - 3: **for** $i = 2, 3, \dots, S_p$ **do**
 - 4: sample a scene point cloud C from paired training samples.
 - 5: acquire P and L of C .
 - 6: use Algorithm A1 with $\{P, L, B\}$ as inputs to synthesize $\{D^{aug}, O_{1:B}^{aug}, p_{1:B}^{aug}\}$.
 - 7: use $\{P, L, D^{aug}, O_{1:B}^{aug}, p_{1:B}^{aug}\}$ to update ϕ with L_{pre} .
 - 8: **end for**
 - 9: $L_{train} \leftarrow \{\mathcal{L}_{text}, \mathcal{L}_{mask}, \mathcal{L}_{ref}\}$
 - 10: **for** $i = 2, 3, \dots, S_o$ **do**
 - 11: sample a data point $\{C, D\}$ in the training samples
 - 12: acquire P and L of C .
 - 13: apply LLM to acquire $O_{1:B}$.
 - 14: use $\{P, L, D, O_{1:B}\}$ to update ϕ with L_{train} .
 - 15: **end for**
-

NR3D For NR3D, we use pre-trained Pointnet++ to classify all object proposals as object labels L following BUTD-DETR [21]. We pre-train DOrA for 15k steps on ScanNet scene point cloud and our augmented samples in Sec. 3.4 and continue on real-world pairs in NR3D for 120k steps using a batch size of 24.

ScanRefer For ScanRefer, since ground-truth object proposals are unavailable, we adopt the visual encoder of M3DRef-CLIP [52] that adopts PointGroup [22] to perform object segmentation as proposals P and object classification as labels L . However, We do not perform object-aware pre-training for ScanRefer since imperfect object proposals may lead to noisy synthetic samples and therefore hinder the training stability of DOrA.

Baselines For baselines [2, 5, 8, 17, 20, 21, 31, 44, 46, 52, 53] on NR3D and ScanRefer in Table 1, 2, and 3, we utilize their official public implementations with different amounts of available training samples and the full testing set to

evaluate their low-resource performance. For the full-data (100%) scenario, we acquire their performance either on the official leaderboard of NR3D/ScanRefer or their published papers. Especially, the implementation of CORE-3DVG [44] is currently unavailable, so we only report its full-data ScanRefer performance, which is presented in their paper. On the other hand, CoT3DRef [5] does not release the parsed datasets required to train their referential-order-based framework, so we only report its performance under settings of full- and 10% training data, which are presented in their original paper.

B Prefix Prompt Examples of Two-Stage ICL for Deriving Referential Order

This section lists the complete prompts of our two-stage ICL using GPT-3.5-Turbo [48] for referential order generation in Sec. 3.2. Also, we exhibit parsing results of 4 samples in the NR3D testing set and compare with CoT3DRef [5] that also establishes the extraction and usage of referential order.

B.1 Prefix Prompt of First-Stage ICL

The first-stage prompt in Sec. 3.2 is used to acquire the summarized description D' and target object O_B of the original description. Our first-stage prompt is as follows:

I have some descriptions, each describing a specific target object in a room. However, they may have some redundant clauses or words. Your task is to summarize them into a shorter description. Also tell me what is the target object. Below are 10 examples:

description 1: *Assume you are facing the door in the room, find the larger cabinet to its left.*

summarized description 1: *When facing the door, the cabinet on the right of it.*

target object 1: *cabinet*

description 2: *The water bottle that is above the easy chair. NOT the smaller water bottle that is above the orange table.*

summarized description 2: *The water bottle that is above the easy chair.*

target object 2: *water bottle*

description 3: *In the bedroom, you will see a sheer curtain, beside the curtain is the steel window you need to find.*

summarized description 3: *The steel window beside a sheer curtain.*

target object 3: *window*

description 4: *Please find the towel hanging on the wall in the bathroom with other three towels. You should find the one which is nearest to the door. Or say it is on the door's right side.*

summarized description 4: *The towel on the wall nearest to the door.*
target object 4: *towel*

description 5: *Between a pencil and a desk lamp on the desk is the backpack you need to find.*

summarized description 5: *The backpack between a pencil and a desk lamp on the desk.*

target object 5: *backpack*

description 6: *In the living room we have three bookshelves. Choose the bookshelf to the right of the clock facing a cabinet.*

summarized description 6: *The bookshelf to the right of the clock facing a cabinet.*

target object 6: *bookshelf*

description 7: *The person wearing a white T-shirt, not the man who is also sitting on the bed but with a jacket.*

summarized description 7: *The person wearing a white T-shirt on a bed.*

target object 7: *person*

description 8: *The purple pillow on the right side of the bed on when facing it. Not the one the left side and the one on the middle of the bed.*

summarized description 8: *The purple pillow on the right side of the bed when facing it.*

target object 8: *pillow*

description 9: *The brown door at the end of the living room, next to the trash cans which is full of garbage.*

summarized description 9: *The brown door next to the full trash can.*

target object 9: *door*

description 10: *The shoes that is placed in the middle of five shoes near the door in the room.*

summarized description 10: *The middle shoes near the door.*

target object 10: *shoes*

Now for the description [DESCRIPTION], give me the summarized description and the target object. Your answer must be in the form "summarized description: target object:"

B.2 Prefix Prompt of Second-Stage ICL

The second-stage prompt in Sec. 3.2 is used to acquire the referential order $O_{1:B}$ based on the target object O_B and the summarized description D' . The complete prompt is as follows:

I have some descriptions, each describing a specific target object with some supporting anchor objects helping the localization. We can find the specific target object by tracing the referential order of anchor objects step by step. Your task is to provide a correct referential order. Also tell me what are the mentioned anchor objects.

Below are 10 examples:

description 1: *The water bottle that is above the easy chair.*

target object 1: *water bottle*

anchor objects 1: *easy chair*

referential order 1: *easy chair->water bottle*

description 2: *The steel window beside a sheer curtain.*

target object 2: *window*

anchor objects 2: *curtain*

referential order 2: *curtain->>window*

description 3: *The trash can that is on the right of the king size bed.*

target object 3: *trash can*

anchor objects 3: *bed*

referential order 3: *bed->trash can*

description 4: *The backpack between a pencil and a desk lamp. They are all on a wooden desk.*

target object 4: *backpack*

anchor objects 4: *pencil, desk lamp, desk*

referential order 4: *desk->pencil->desk lamp->backpack*

description 5: *The cabinet on the right of the door.*

target object 5: *cabinet*

anchor objects 5: *door*

referential order 5: *door->cabinet*

description 6: *The bookshelf to the right of the clock facing a cabinet.*

target object 6: *bookshelf*

anchor objects 6: *clock, cabinet*

referential order 6: *cabinet->clock->bookshelf*

description 7: *The person wearing a white T-shirt on a bed.*

target object 7: *person*

anchor objects 7: *bed*

referential order 7: *bed->person*

description 8: *The purple pillow on the right side of the bed when facing it.*

target object 8: *pillow*

anchor objects 8: *bed*

referential order 8: *bed->pillow*

description 9: *The brown door next to the full trash can.*

target object 9: *door*

anchor objects 9: *trash can*

referential order 9: *trash can->door*

description 10: *Please find the towel hanging on the wall in the bathroom with other three towels. You should find the one nearest to the door. Or say it is on the door’s right side.*

target object 10: *towel*

anchor objects 10: *wall, door*

referential order 10: *wall->door->towel*

Now for the description: [DESCRIPTION], give me the anchor objects and the referential order. Your answer must be in the form "referential order: , anchor objects: ".

B.3 Examples of Derived Referential Order

To show that our two-stage ICL produces reasonable referential orders, we provide examples and comparisons between ours and CoT3DRef [5]’s parsing results. Note that CoT3DRef currently does not release their complete parsing results of NR3D, so we manually leverage its released prompt files in their paper and official repository to query the GPT-3.5-Turbo. We display 4 examples in Tab. A5, where CoT3DRef misses an anchor object “*bed*” in the third example and includes a redundant object “*shelves*” as an anchor object in the fourth example, while our DOrA produces proper results in both cases. This shows the effectiveness of two-stage ICL strategy.

C Ablation Studies on Training Objectives

This section performs the ablation study on several training objectives used for DOrA mentioned in Sec. 3. In particular, we investigate the influence of \mathcal{L}_{mask} , \mathcal{L}_{crd} , and \mathcal{L}_{text} for low-resource (1% training data) and full-resource (100% training data) scenarios, as shown in Tab. A6. Note that we only conduct target object classification on the text feature T when deactivating \mathcal{L}_{text} , and apply classification on both anchor and target objects when adopting \mathcal{L}_{text} , as mentioned in Sec. 3.3. Also, for all experiments in Tab. A6, the pre-training with synthetic data in Sec. 3.4 is applied for fair comparison. In summary, \mathcal{L}_{mask} , \mathcal{L}_{crd} , and \mathcal{L}_{text} all impose positive effects on models’ performances under the two settings, verifying DOrA’s design in Sec. 3.

Table A5: Examples of LLM-parsed referential order from CoT3DRef [5] and DOrA. Note that the blue text represent the ideal anchor/target objects and the red text represent the redundant object that should not appear in the referential order. We can see that MVT misses one anchor object in the third example and includes a redundant object in the fourth example, while DOrA predicts proper order for both cases.

Description	CoT3DRef [5]	DOrA (Ours)
The pillow closest to the foot of the bed .	bed -> pillow	bed -> pillow
Facing the bed , it's the large white pillow on the right. The second one from the headboard .	bed -> headboard -> pillow	bed -> headboard -> pillow
The front pillow on the bed with the laptop .	bed -> pillow	laptop -> bed -> pillow
The window near the table , not the one near the shelves .	table -> shelves -> window	table -> window

Table A6: Ablation studies on training objectives. Note that for all ablated settings, the proposed order-aware pre-training in Sec. 3.4 is applied for fair comparison.

\mathcal{L}_{mask}	\mathcal{L}_{crd}	\mathcal{L}_{text}	\mathcal{L}_{ref}	1%	100%
			✓	31.1	54.2
		✓	✓	31.6	54.8
	✓	✓	✓	32.4	56.0
✓	✓	✓	✓	33.5	59.7

D Model Performance Under Different Order Length

This section explores DOrA’s performance gain for descriptions with different order lengths compared with MVT [20] to show the effectiveness of our design of progressive location to the target object. We split the original NR3D testing set into subsets that possess order lengths of **1**, **2&3**, and **4&5**. An order length of 1 (1092 samples in the testing set) means that only the target object is mentioned in the description. Samples with an order length of 2 or 3 (6184 samples in the testing set) have 1 or 2 anchor objects mentioned other than the target object. Similarly, samples with an order length of 4 or 5 (209 samples in the testing set) have 3 or 4 anchor objects mentioned other than the target object. A longer referential order may generally denote a longer and more complicated description. As shown in Tab. A7, though only a 2.2% performance gain is obtained for target-only samples, DOrA is more advantageous when dealing with lengthy descriptions, with 5.3% performance gain achieved for descriptions with order length of 4 or 5.

Table A7: Grounding accuracy on NR3D subsets regarding different parsed referential order lengths. Note that referential order length = 1 means only the target object is mentioned in the description. The improvement of DOrA over MVT [20] grows as the parsed order length increases.

Method	Order Length			overall
	1	2&3	4&5	
MVT [20]	59.4	55.0	46.7	55.1
DOrA (Ours)	61.6 (+2.2)	59.6 (+4.6)	52.0 (+5.3)	59.7 (+4.6)

E Visualization of Responses in Each Referring Block

To show that our DOrA indeed progressively locates the target object following the derived referential order, we visualize the feature response of $F_{1:(B+1)}$ ($B = 4$) in Fig. A6. The blue bounding box indicates the ground-truth target object, and we color the object proposal according to the response of their corresponding features in $F_{1:(B+1)}$, where a brighter color represents a higher response. We can see that the responses to object proposals are originally cluttered. As our referential blocks are applied, the response of anchor/target objects becomes larger and finally locates the ideal target object in the last feature F_5 .

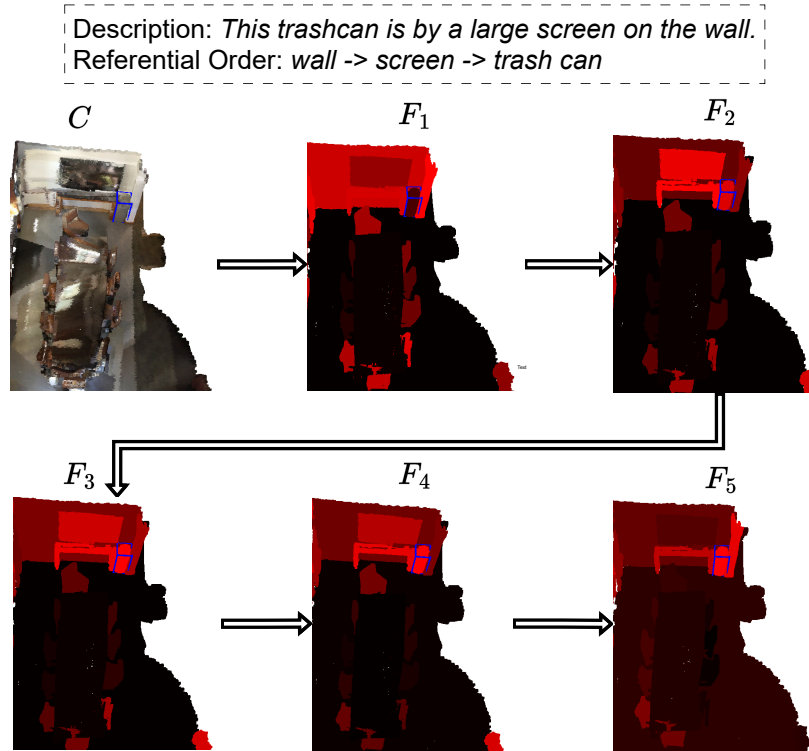


Fig. A6: Visualization of Responses in Each Referring Block. An example in NR3D is shown in this figure. We color each object proposal according to their feature response in $F_{1:(B+1)}$, where larger response with brighter color. Note that the blue bounding box represents the ground truth target object. We can see that our DOrA progressively locate the target object by considering the referential order by first focus the wall then the screen and finally the trash can.